ATP Binding Causes a Conformational Change in the γ Subunit of the *Escherichia coli* F_1ATPase Which Is Reversed on Bond Cleavage†

Paola Turina and Roderick A. Capaldi*

Institute of Molecular Biology, University of Oregon, Eugene, Oregon 97403

Received August 12, 1994; Revised Manuscript Received September 27, 1994®

ABSTRACT: ATP hydrolysis by the *Escherichia coli* F_1 ATPase (ECF_1) induces a conformational change in the γ subunit. This change can be monitored by fluorescence changes in *N*-[4-[7-(diethylamino)-4-methyl]coumarin-3-yl)]maleimide (CM) bound at a cysteine introduced by site-directed mutagenesis into the γ subunit at position 106 [Turina, P., & Capaldi, R. A. (1994) *J. Biol. Chem. 269*, 13465−13471]. In studies reported here, the magnitude of the fluorescence change has been determined with the noncleavable nucleotide analogue AMP•PNP and by rapid measurements using the slowly cleavable ATPγS. The data indicate that maximal fluorescence change occurs with binding of 1 mol of nucleotide triphosphate per mole of ECF_1. During unisite catalysis, ATP binding causes a fluorescence enhancement from CM bound at position 106, which is then followed by fluorescence quenching. The kinetics of these fluorescence changes have been measured using both ATP and ATPγS as substrate. With ATPγS, these kinetics can be simulated using rate constants similar to those for ATP except for an approximately 30-fold slower rate of the bond cleavage and resynthesis steps, i.e., k_{+2} and k_{-2}. The observed rates and amplitudes of the fluorescence changes on hydrolysis of ATP and ATPγS were analyzed by simulations in which the bond cleavage or the P_i release step was responsible for fluorescence quenching. The results indicate that ATP or ATPγS binding causes the fluorescence enhancement of CM bound to the γ subunit and that this conformational change is reversed upon bond cleavage to yield ADP•P_i or ADP•P_iS in catalytic sites.

F_1F_0 type ATPases function both to synthesize ATP from ADP plus P_i in the presence of a light-driven or respiratory-chain generated proton gradient and as ATPases, using the hydrolysis of ATP to establish a pH gradient for subsequent use in ion or substrate transport. The simplest F_1F_0 ATPases structurally are those for bacteria. The *Escherichia coli* enzyme (ECF_1F_0)[1] is a complex of eight different subunits. The F_1 part contains five subunits α, β, γ, δ, and ϵ in the molar ratio 3:3:1:1:1, while the F_0 part contains subunits a, b, and c in the molar ratio 1:2:10−12 [reviewed by Cross (1988) and Senior (1990)].

We have been studying nucleotide-dependent structural change in ECF_1 by incorporating Cys residues into the enzyme by site-directed mutagenesis and using these as the sites for reaction of reporter groups (e.g., Aggeler & Capaldi, 1992; Aggeler *et al.*, 1992, 1993; Wilkens & Capaldi, 1994; Turina & Capaldi, 1994). In recent experiments we showed that the fluorescence of CM bound at a Cys at residue 106 of the γ subunit responded to ATP hydrolysis in catalytic sites (Turina & Capaldi, 1994). When ATP was bound under conditions for unisite catalysis, there was a fluorescence enhancement of the CM at this site which was followed by a fluorescence quenching. The kinetics of these fluorescence changes followed closely the kinetics of unisite catalysis, indicating that the structural changes being observed are linked to ATP hydrolysis in catalytic sites. From these earlier experiments it was clear that ATP binding induced a structural change in the γ subunit but it was not obvious at which step in ATP hydrolysis, i.e., bond cleavage or P_i release, the structural change was reversed.

To examine this issue further, we have studied the fluorescence changes in the presence of AMP•PNP, ATPγS, as well as ATP, as a function of the nucleotide concentration. By determining the maximal fluorescence enhancement on binding of these substrates, which proved to occur when 1 mol bound per mole of ECF_1, we have been able to examine the fluorescence changes quantitatively. This information, along with measurements on the rates of fluorescence change using ATP, and particularly ATPγS, have allowed us to distinguish between bond cleavage and P_i release as the step at which fluorescence quenching occurs.

MATERIALS AND METHODS

CM was obtained from Molecular Probes. ATP, ADP, and pyruvate kinase were from Sigma. ATPγS, AMP•PNP, and phosphoenolpyruvate were from Boehringer Mannheim. [γ-^{32}P]ATP was purchased from Amersham Corp. and [^{35}S]-ATPγS from DuPont Biotechnology Systems. The mutant of ECF_1 used in this study, γT106-C, was generated as described in Aggeler and Capaldi (1992). ECF_1 was isolated from the *E. coli* mutant by a modification of the method of Wise *et al.* (1981), described in Gogol *et al.* (1989). Purified enzyme was stored under liquid nitrogen. Prior to use, ECF_1 was routinely precipitated with 70% ammonium sulfate at 4 °C, dissolved in buffer A (50 mM MOPS/HCl, 0.5 mM

† Supported by National Institutes of Health Grant HL 24526.

* To whom correspondence should be addressed at the Institute of Molecular Biology, University of Oregon, Eugene, OR 97403-1229. Telephone: (503) 346-5881. Fax: (503) 346-4854.

® Abstract published in *Advance ACS Abstracts,* November 1, 1994.

[1] Abbreviations: CM, *N*-[4-[7-(diethylamino)-4-methyl]coumarin-3-yl]maleimide; ECF_1, soluble portion of the *E. coli* F_1F_0 ATPsynthase; ATPγS, adenosine-5′-*O*-(3-thiotriphosphate); AMP•PNP5′-adenylylimidodiphosphate; MOPS, 3-(*N*-morpholino)propanesulfonic acid; HEPES, *N*-(2-hydroxyethyl)piperazine-*N*′-(2-ethanesulfonic acid); EDTA, ethylenediaminetetraacetic acid.

0006-2960/94/0433-14275$04.50/0

EDTA, 10% glycerol, pH 7.0), and passed once through a centrifuge column (Penefsky, 1977) equilibrated in the same buffer.

The concentrations of ATP, ATPγS, and AMP·PNP stock solutions in buffer B were determined from their absorbance at 259 nm using an extinction coefficient of 15.4×10^3 M^{-1} cm^{-1}. For ATPγS solutions, only 90% of this absorption was taken to be due to ATPγS, since a 10% ADP content is indicated by the company. Molar concentrations of ECF_1 were estimated with the BCA protein assay from Pierce Chemicals using a molecular weight of 382 000.

CM Labeling of the Introduced Cys Residue in ECF_1. CM labeling was performed as described in Turina and Capaldi (1994). Close to stoichiometric concentrations of CM and short reaction times (30 s^{-1} min) routinely yielded specific labeling of the introduced Cys residue in the γ subunit, as confirmed by SDS−polyacrylamide gel electrophoresis. The labeled enzyme was stored under liquid nitrogen. Before use, thawed aliquots of the labeled ECF_1 were diluted to a concentration of 4 μM in buffer B (50 mM HEPES/NaOH, 0.5 mM EDTA, 2.5 mM $MgCl_2$, pH 8.0) and equilibrated in this buffer for at least 1 h. The enzyme was then diluted in buffer B to the final concentration just shortly before starting the activity of fluorescence measurements.

Assays of ATP and ATPγS Hydrolysis. The hydrolysis reactions were started by mixing the enzyme solution in buffer B with an equal volume of the same buffer containing [γ-^{32}P]ATP or [^{35}S]ATPγS (100−150 kBq/mL) to give final enzyme concentrations 3−6-fold in excess of nucleotide. The reactions were quenched at different time points with a 10% (w/v) trichloroacetic acid solution containing 1 mM cold nucleotide. The mixing steps were carried out at room temperature (21−22 °C) either by rapid manual operation under stirring or in a quench-flow apparatus ("System 1000" from Update Instrument Inc.).

The samples containing [γ-^{32}P]ATP were analyzed for [^{32}P]P_i content by organic solvent extraction of the phosphomolybdate complex and/or by the charcoal adsorption assay using 50 mM KH_2PO_4 as carrier salt. The two methods resulted in identical rates of ATP hydrolysis. The samples containing [^{35}S]ATPγS were analyzed for [^{35}S]S content by the charcoal adsorption assay using 50 mM Na_3PO_3S as carrier salt.

The background radioactivity which was not charcoal adsorbed was determined by mixing the enzyme solution with the trichloroacetic acid solution before addition of radioactive nucleotide. The data were also corrected for the amount of nonhydrolyzable background, present as charcoal adsorbed radioactivity after ATP or ATPγS hydrolysis was carried out to completion (10 μM−1 mM nucleotide reacted for about 1 h).

Measurements of CM Fluorescence. The fluorescence measurements were performed at room temperature using an SLM 8000 photon counting spectrofluorometer. The volume of the samples was 300 μL in a 0.4 × 1-cm quartz cuvette. The CM was excited at 395 nm. All signals were recorded as a ratio of the emission and excitation channels and were routinely corrected for the background signal of buffer with unlabeled protein and for dilution effects.

The difference between the spectrum of enzyme in the absence of nucleotide and that of ECF_1 with bound ATPγS (Figure 2A) was obtained by performing a series of independent measurements, in which the same nucleotide addition giving the maximal effect was repeated at a number of different wavelengths. The emission fluorescence was recorded simultaneously in the two emission channels, one of which was kept at a constant wavelength, in order to correct for the small variability among different samples.

For unisite measurements, 30 μL of nucleotide solution was routinely added with a Hamilton syringe and rapidly mixed with a plastic rod. Data were recorded with an integration time of 100 ms and smoothed after the acquisition. During the course of this work it was noticed that the signals obtained at the highest concentration of reactants (1 μM ECF_1 and 0.3 μM ATP or ATPγS) were systematically slightly lower than expected and could be simulated well by using a concentration of nucleotide 10−15% lower than the nominal concentration. We hypothesized that at this high concentration a fraction of the added nucleotide was binding to a site where hydrolysis did not occur, e.g., a so-called noncatalytic site. To prevent this, when 1 μM enzyme was used, stoichiometric amounts of ADP were added to the solutions 5 min before starting the reaction to fill the competing site. After this treatment, the signals could be satisfactorily simulated using values for the added concentrations of nucleotides. At the lower concentrations of enzyme, pretreatment with ADP did not affect the appearance of the fluorescence signals and was therefore routinely omitted.

Kinetic Analysis. Simulations of the kinetics of unisite catalysis by ECF_1 were performed by the software system KINSIM (Barshop *et al.*, 1983) on a VAX 3000 computer. This software generates a system of differential equations describing the kinetic mechanism given as input and performs a numerical integration. The kinetic mechanism used for ATP was the following, according to Grubmeyer *et al.* (1982):

$$F_1 + ADP \underset{k_{-1}}{\overset{k_{+1}}{\rightleftharpoons}} F_1{\cdot}ATP \underset{k_{-2}}{\overset{k_{+2}}{\rightleftharpoons}} F_1{\cdot}ADP{\cdot}P_i \underset{k_{-3}}{\overset{k_{+3}}{\rightleftharpoons}} F_1{\cdot}ADP + P_i \underset{k_{-4}}{\overset{k_{+4}}{\rightleftharpoons}} F_1 + ADP \quad (1)$$

k_{+4} and k_{-4} do not affect the rate of P_i formation or the time courses of fluorescence signals, and k_{-1} and k_{-3} are comparatively very small, such that they can be neglected.

RESULTS

Hydrolysis Rates with ATPγS as Substrate. ATPγS has been used to study the kinetics of a number of ATPases, all of which turn over more slowly with this substrate than with ATP because of impaired cleavage of the thiophosphate bond (Bagshaw *et al.*, 1972; Webb *et al.*, 1980; Thompson & Karim, 1982; Eckstein, 1983). Figure 1 compares the initial rates of hydrolysis of ATPγS and ATP, measured under unisite conditions, with both rapid quench and manual mixing methods, using ECF_1 from the mutant of γT106C. In this, and all activity measurements in this study, the mutant was reacted first with CM in order to maintain the conditions used in fluorescence measurements (see later). A clear lag in the rate of P_iS formation was observed with ATPγS as substrate; this was not seen for P_i formation from ATP. Previously, we could describe the rate of ATP hydrolysis under unisite conditions using the mechanism (eq 1) and set of rate constants listed in Table 1 (Turina & Capaldi, 1994). The line drawn through the data for ATP hydrolysis was generated using these same rate constants.

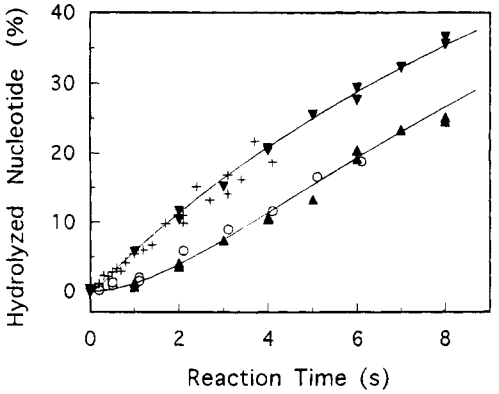

FIGURE 1: ATP and ATPγS hydrolysis by CM-labeled ECF_1 from γT106-C under unisite conditions. The reactions were carried out as described under Materials and Methods with an enzyme concentration of 260 nM. (▼, +) The nucleotide was [γ -^{32}P]ATP, at concentrations of 80 nM (▼) or 45 nM (+). (▲, ○) The nucleotide was [^{32}S]ATPγS, at a concentration of 80 nM. (▼, ▲) Manual operation; (+, ○) quench-flow. The lines through the points represent the expected percentage of hydrolyzed nucleotide as a function of time, according to the mechanism and rate constants reported under Materials and Methods. For ATP, only the expected percentage at 80 nM nucleotide is reported, the percentage at 45 nM differing only marginally.

Table 1: Rate Constants of Unisite Catalysis of ATP and ATPγS

		ATPγS	
	ATP[a]	simulated[b]	range by curve fitting[c]
k_{+1} (M^{-1} s^{-1})	3.9×10^5	3.9×10^5	$(3.6-4.4) \times 10^5$
k_{+2} (s^{-1})	8.2	0.27	0.16−0.35
k_{-2} (s^{-1})	4.4	0.15	0.19−0.22
k_{+3} (s^{-1})	3.4×10^{-2}	3.4×10^{-2}	$(3-5) \times 10^{-2}$

[a] From Turina and Capaldi (1994). [b] Simulating the ATPγS hydrolysis and fluorescence data by modifying only k_{+2} and k_{-2}. [c] Obtained by solving exactly the set of differential equations derived from the kinetic mechanism of eq 1 reported under Materials and Methods. A narrow range for each variable gave an adequate fit to the experimental data.

A lag in P_iS formation with ATPγS as substrate would be expected if the rates of cleavage and resynthesis are slow enough with respect to the binding of the nucleotide, because of initial accumulation of uncleaved ATPγS on the enzyme. For a first analysis, only k_{+2} and k_{-2} were varied, and, as shown in Figure 1, the rate of generation of P_iS could be predicted very well using values of the rates of ATPγS cleavage and resynthesis that are 30-fold lower than those for ATP (Table 1), while leaving the same rate constants for substrate binding and release of product that were used for ATP.

Binding of ATPγS, AMP•PNP, and ATP Measured by Fluorescence Enhancement. The binding of ATPγS to CM-labeled ECF_1 from the mutant γT106C caused a rapid fluorescence enhancement followed by a slower fluorescence quenching as the substrate was hydrolyzed to ADP and P_iS, a result similar to that obtained on binding ATP. When the extent of this initial fluorescence enhancement was titrated as a function of ATPγS concentration, a maximum was reached between 10 and 15 μM. By recording the maximum fluorescence enhancement at a number of different wavelengths, a difference spectrum could be obtained, as shown in Figure 2A (solid circles). In the same figure, the difference spectra induced by saturating concentrations of

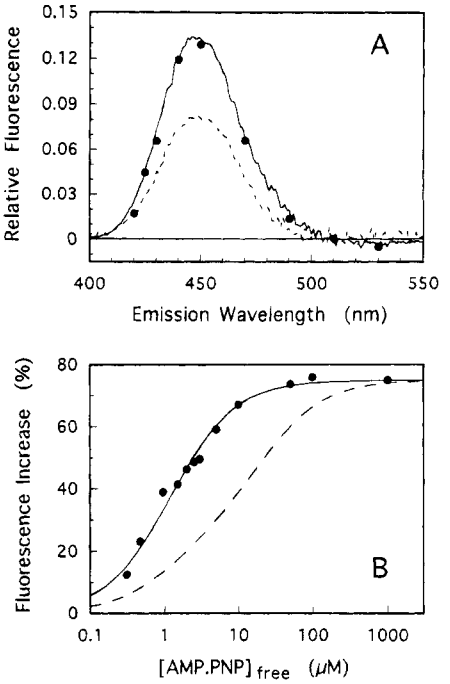

FIGURE 2: AMP•PNP, ATP, and ATPγS induced fluorescence changes in CM-labeled ECF_1 from γT106-C. (Panel A) The solid line is the difference between the emission spectra of CM bound to ECF_1 (100 nM) recorded in the presence and in the absence of 50 μM AMP•PNP. The dashed line is the difference between the emission spectra of CM bound to ECF_1 (50 nM) in the presence and in the absence of 10 μM ATP; also present were 100 units/mL pyruvate kinase, 10 mM phosphoenolpyruvate, and 10 mM KCl as ATP-regenerating system in order to stabilize the signal during the time required to record the spectrum. The solid circles are the difference between the emission fluorescence recorded at each indicated wavelength in the first seconds after the addition of 15 μM ATPγS and the emission fluorescence recorded at the same wavelength before the addition. (Panel B) AMP•PNP titration of the change in fluorescence emission recorded at 430 nm of CM bound to ECF_1. The enzyme concentration was 100 nM. The solid line describes the binding curve expected for a single K_d of 1.2 μM. The dashed line describes, for comparison, the binding curve expected for three sites with K_ds of 1.2, 30, and 30 μM, respectively, with each site responsible for one-third of the total fluorescence enhancement. For each concentration, the time course of fluorescence increase upon addition of AMP•PNP was recorded as a function of time until no further significant change occurred; each of these time courses could be well described by a reversible second-order reaction with association rate constant of 2.2×10^3 M^{-1} s^{-1} and dissociation rate constant of 2.7×10^{-3} s^{-1}.

the noncleavable AMP•PNP (solid line) and ATP (dashed line) are also reported.

It can be seen that the spectral shift obtained with ATPγS is the same as obtained with ATP or AMP•PNP. Moreover, the maximal fluorescence enhancement with ATPγS is the same as obtained with AMP•PNP bound. By comparison with both the noncleavable and slowly cleavable analogues, the lower fluorescence enhancement obtained with high concentrations of ATP (as high as 1 mM), even in the presence of an ATP regenerating system, can be best explained if the rapid cleavage rate leads to an immediate equilibration of ATP and ADP on the enzyme. From these data, we conclude that the three nucleotides induce the same conformational change in the γ subunit.

The nucleotide concentration dependence of the fluorescence enhancement for AMP•PNP is shown in Figure 2B. The curve can be fitted by a binding curve with a single K_d of 1.2 μM. In the case of AMP•PNP, it has been shown by

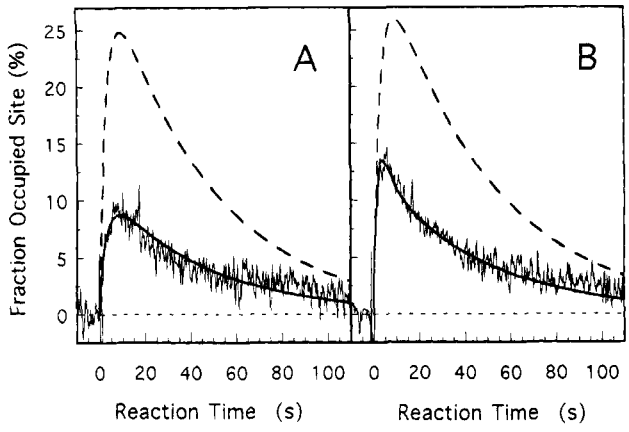

FIGURE 3: Fluorescence changes induced in CM-labeled ECF_1 from γT106C by ATP and ATPγS unisite hydrolysis. The enzyme concentration was 1 μM. The fluorescence emission was recorded at 430 nm as a function of time. At time = 0, 305 nM ATP (panel A) or 305 nM ATPγS (panel B) was added. The fluorescence signals were converted to fraction of occupied site by taking as 100% occupancy the maximum fluorescence enhancement recorded at the same wavelength with saturating concentrations of AMP•PNP (75%, see Figure 2B). The solid lines represent the enzyme fraction expected to be in the F_1•ATP state (panel A) or F_1•ATPγS (panel B) according to the mechanism and reaction constants reported under Materials and Methods. The dashed lines represent the enzyme fraction expected to be in both states F_1•ATP and F_1•ADP•P_i (panel A) or F_1•ATPγS and F_1•ADP•P_iS (panel B) according to the mechanism of eq 1 and reaction constants reported in Table 1.

two very different methods [binding equilibrium assays (Wise *et al.*, 1983) and using the mutant βY331W (Weber *et al.*, 1993)], that this ATP analogue binds to ECF_1 in three catalytic sites, one with a high affinity (K_d around 0.3 μM), the other two with a K_d of 20 μM or greater. The value of 0.3 μM for the tight site is close to the K_d from the nucleotide-induced fluorescence change measured here, as we are using a CM-modified mutant enzyme. We conclude that the fluorescence changes we are observing are due to binding at the (single) high affinity catalytic site. Further, we must conclude that there are no further fluorescence changes due to binding in additional catalytic sites, i.e., the enzyme shows one-third of site activity for nucleotide-induced structural changes in the γ subunit. Similarly, with both ATPγS and ATP, the observed fluorescence changes must be due to binding only to the high affinity catalytic site. In the following, the maximum extent of fluorescence enhancement seen with AMP•PNP and ATPγS is, therefore, taken as 100% occupancy of the high affinity site.

Kinetics of the Fluorescence Changes on Hydrolysis of ATPγS and ATP. The fluorescence enhancement caused by ATP (or ATPγS) binding is followed by fluorescence quenching as the nucleotide triphosphate is converted to ADP and P_i (or P_iS). This quenching could be due to bond cleavage, with bound ATP giving a higher fluorescence than ADP•P_i, or due to P_i release with both bound ATP and ADP•P_i generating the high fluorescence state. Figure 3A shows the observed time course of fluorescence change on reacting 1 μM ECF_1 with 0.3 μM ATP. Also shown are simulations of this time course using the rate constants in Table 1, assuming that the fluorescence quenching is due to bond cleavage (solid line) and P_i release (dashed line). The shape of the two simulated curves is identical, but the maximal fluorescence enhancement expected is very different in the two cases. From Figure 3A it can be seen that the data best fit a mechanism in which bond cleavage causes fluorescence quenching. Figure 3B shows data for reaction of ECF_1 (1 μM) with ATPγS (0.3 μM) and simulation with a mechanism in which bond cleavage (solid line) or P_iS release (dashed line) causes the fluorescence quenching. As discussed above, during the lag phase (Figure 1), uncleaved ATPγS accumulates on the enzyme, and the ratio of uncleaved versus cleaved nucleotide is temporarily much higher than the ratio expected once the equilibrium between ATPγS and ADP•P_iS has been established. The implication is that, in the early times of unisite catalysis with ATPγS as substrate, the concentrations of F_1•ATPγS and F_1•ADP•P_iS will have a different shape as a function of time (this is not the case for F_1•ATP and F_1•ADP•P_i, as shown in Figure 3A). Thus at 1 μM F_1 with 0.3 μM ATPγS and using the rate constants in Table 1, the species F_1•ATPγS will reach a maximum and then decline at 4 s, but the sum of the species F_1•ATPγS + F_1•ADP•P_iS will not reach a maximum until 10 s. These two cases are shown by the solid line and dotted line, respectively. As evident in Figure 3, the data obtained for ATPγS follow well *both* the rate dependence and concentration dependence of fluorescence change expected for fluorescence quenching caused by the bond cleavage reaction.

A mechanism of fluorescence change in which bond cleavage causes the quenching also fits data collected at lower concentrations of ECF_1 and ATPγS (but keeping the ratio of the two the same) when the ATPγS binding rate becomes more important. Such data are shown in Figure 4. The rates of fluorescence quenching for ATP and ATPγS proved to be similar once all the substrate had bound and the equilibrium ATP (or ATPγS) to ADP•P_i (or ADP•P_iS) had been established. In this phase of the reaction, the rate of shifting from the high fluorescence state (ATP or ATPγS bound) to the low fluorescence state (ADP•P_i or ADP•P_iS bound) becomes dependent on the rate of P_i release. The data in Figures 3 and 4 are evidence that this rate is very similar for P_i and P_iS.

For simplicity, the data of Figure 1 above for ATPγS hydrolysis were analyzed by varying only the rates of bond cleavage and resynthesis (k_{+2} and k_{-2}). The good fit to both pre-steady-state activity data (Figure 1) and to the nucleotide-induced fluorescence changes validates this approach. However, a more rigorous analysis of the fitting of theoretical rate curves to observed data was possible, and this was done. Briefly, a system of differential equations was derived from the mechanism in eq 1. This system can be solved exactly, e.g., by using the Laplace–Carson operator method [see Roberts (1977)] with the approximation that the enzyme concentration remains constant throughout the reaction. A three-exponential function is generated, whose relaxation times and amplitudes are a function of the four kinetic constants, k_{+1}, k_{+2}, k_{-2}, and k_{+3}, along with enzyme and substrate concentrations.

A maximum of four independent parameters characterizes this function. These four parameters are determined unequivocally when the three differently shaped fluorescence traces obtained at different concentrations of ATPγS are fully described in terms of their rates and relative amplitudes. The values of the kinetic constants obtained by fitting the four parameters to the fluorescence traces validated the rate constants deduced by the simpler approach described earlier (Table 1).

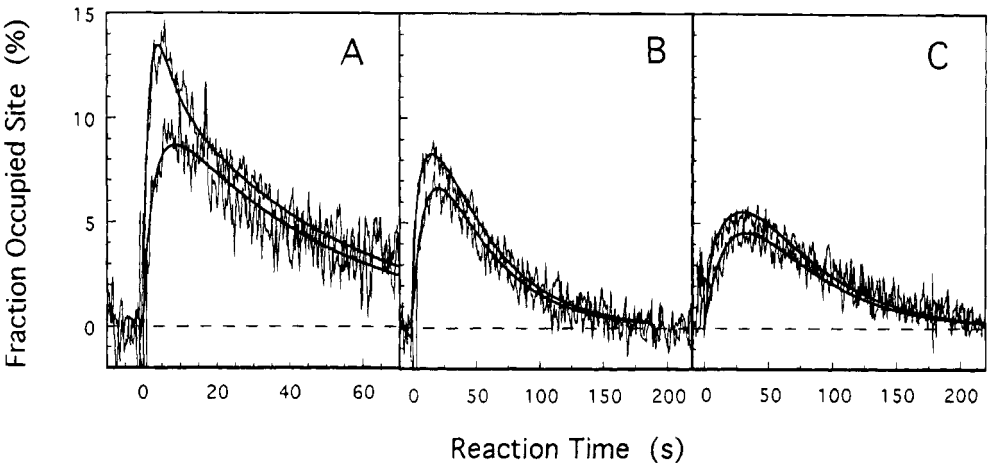

FIGURE 4: Fluorescence changes induced in CM-labeled ECF_1 from γT106C by ATP and ATPγS unisite hydrolysis at various enzyme and substrate concentrations. The fluorescence emission was recorded at 430 nm as a function of time. The nucleotides were added at time = 0. The signals were converted in fraction of occupied site by taking as 100% occupancy the maximum fluorescence enhancement recorded at the same wavelength with saturating concentrations of AMP·PNP (75%, see Figure 2B). The traces of Figure 3 are reported again for better comparison. (Panel A) 1 μM enzyme, 305 nM ATP (lower trace) or ATPγS (upper trace). (Panel B) 260 nM enzyme, 80 nM ATP (lower trace) or ATPγS (upper trace). (Panel C) 105 nM enzyme, 30 nM ATP (lower trace) or ATPγS (upper trace). The solid lines represent the enzyme fraction expected to be in the state F_1·ATP or F_1·ATPγS according to the mechanism of eq 1 and reaction constants reported in Table 1.

DISCUSSION

The results presented here show that ATP binding in catalytic sites causes a conformational change in the γ subunit and that ATP hydrolysis reverses this change in a time course that follows bond cleavage rather than P_i release. The fluorescence enhancement seen on adding AMP·PNP, ATP, or ATPγS to ECF_1 is clearly a function of the binding of the nucleotide triphosphate into a catalytic site. The maximum fluorescence change occurs when one catalytic site is filled, as shown by the experiments using noncleavable AMP·PNP or slowly cleavable ATPγS. The rate of the subsequent quenching observed with ATP (or ATPγS) as substrate could be due to bond cleavage or to P_i release. Our studies show that it is too fast to be caused by P_i release, and, moreover, the optimal fluorescence enhancement is too low for both of the species F_1·ATP and F_1·ADP·P_i to give the high fluorescence observed. However, both the amplitude of the fluorescence change and the rate of fluorescence quenching fit well with this quenching occurring on conversion of ATP to ADP·P_i in a catalytic site when these parameters are simulated using unisite catalytic rate constants used previously (Turina & Capaldi, 1994). These values for k_{+2} and k_{-2} that describe both the rate of ATP hydrolysis and the rate of fluorescence change (Turina & Capaldi, 1994) are somewhat different from those reported by Al-Shawi and Senior (1992). However, as discussed before (Turina & Capaldi, 1994), our experiments use a mutant ECF_1 which has been modified in the introduced Cys by CM. The CM-labeled enzyme has a higher basal ATPase activity than wild-type enzyme, related at least in part to an altered interaction of the ϵ subunit (C. Tan and R. A. Capaldi, unpublished results). Nevertheless, ECF_1F_0 purified from the mutant retains normal ATP-driven proton pumping function, is therefore coupled, and the conformational change being monitored by the fluorescence studies here and in Turina and Capaldi (1994) can be expected to be the same ones occurring with wild-type ECF_1.

That ATP bond cleavage drives the conformational change in the γ subunit is further supported by data for ATPγS hydrolysis by the enzyme. There is strong evidence that the rate of bond cleavage of ATPγS is slower than that of ATP from data on several ATPases (Bagshaw *et al.*, 1972; Thompson & Karim, 1982; Eckstein, 1983). Consistent with this, the rate of ATPγS hydrolysis measured here under unisite conditions could be modeled by the same set of rate constants as for ATP hydrolysis except for 30-fold slower values of k_{+2} and k_{-2}.

As a consequence of these slower rates of bond cleavage and resynthesis, uncleaved ATPγS would be expected to build up on ECF_1, as compared with ATP, so that the optimal fluorescence enhancement is higher, and this was the case. Using the same rate constants that fitted the rate of ATPγS hydrolysis, it was possible to simulate the amplitude and both the rates of attainment of maximal fluorescence enhancement and fluorescence quenching if the fluorescence quenching was caused by bond cleavage. No good fit to the experimental data could be obtained when P_iS release was considered to cause fluorescence quenching, even when all of the rate constants were systematically varied.

With both ATP and ATPγS, once all of the substrate has bound to the enzyme and an equilibrium established between ATP (or ATPγS) and ADP·P_i (or ADP·P_iS), the rate of fluorescence quenching will be determined by the rate of P_i (or P_iS) release. The observed data at lower concentrations of ATP and ATPγS to ECF_1 show that the off-rate of P_i (k_{+3}) is very similar for both substrates.

Structural studies indicate that the 3α and 3β subunits alternate in a ring surrounding a cavity in which the γ subunit is located (Gogol *et al.*, 1989; Abrahams *et al.*, 1993; Ishii *et al.*, 1993). We have shown that there are nucleotide-dependent conformational changes in the γ subunit based on fluorescence experiments such as described here (Turina & Capaldi, 1994) and in cross-linking studies which also place the N terminus of γ close to (less than 15 Å from) a catalytic site on one of the β subunits (Aggeler & Capaldi, 1992, 1993; Aggeler *et al.*, 1993).

From the kinetic analysis presented here, it is ATP binding in the high affinity site that drives the conformational change

in the γ subunit, which is then reversed on bond cleavage to give ADP·P_i. We have argued that the conformational changes being monitored in our cross-linking and fluorescence experiments are a part of the coupling mechanism (Capaldi *et al.*, 1994). For example, they are lost in ECF_1 from which the ϵ subunit has been removed, although the enzyme is an active and cooperative ATPase (Aggeler & Capaldi, 1993; Turina & Capaldi, 1994). As discussed (e.g., Jencks, 1980; Hammes, 1982; Tanford, 1983; Läuger, 1984), a minimal mechanism of operation of an ion pump requires that the protein assumes at least two main conformational states. In the case of ECF_1 and other F_1 ATPases, the γ subunit in association with the ϵ subunit (or equivalent δ subunit in MF_1) may switch between two conformations seen here (equivalent to the E_1 and E_2 states for other transport ATPases) in response to structural changes in catalytic sites. There may be, in addition, conformational changes in the γ subunit in association with catalytic site cooperativity, for example, translation of this subunit from one catalytic site to another [Gogol *et al.*, 1990; Wilkens & Capaldi, 1994; discussed in Boyer (1993)], which can be uncoupled from the energy transducing conformational transitions being described here. How the structural changes in the γ (and ϵ) subunit are linked to proton translocation in the F_0 remains the critical issue in understanding the mechanism of ATP synthesis by F_1F_0 ATPases.

ACKNOWLEDGMENT

The excellent technical assistance of Kathy Chicas-Cruz is gratefully acknowledged. We thank Dr. B. Andrea Melandri and Dr. Mark Young for helpful discussions.

REFERENCES

Abrahams, J. P., Lutter, R., Todd, R. J., van Raaij, M. J., Leslie, A. G. W., & Walker, J. E. (1993) *EMBO J. 12*, 1775−1780.

Aggeler, R. J., & Capaldi, R. A. (1992) *J. Biol. Chem. 267*, 21355−21359.

Aggeler, R., & Capaldi, R. A. (1993) *J. Biol. Chem. 268*, 14576−14579.

Aggeler, R. J., Chicas-Cruz, K., Cai, S. X., Keana, J. F. W., & Capaldi, R. A. (1992) *Biochemistry 31*, 2956−2961.

Aggeler, R. J., Cai, S. X., Keana, J. F. W., Koike, T., & Capaldi, R. A. (1993) *J. Biol. Chem. 268*, 20831−20837.

Al-Shawi, M. K., & Senior, A. E. (1992) *Biochemistry 31*, 878−885.

Bagshaw, C. R., Eccleston, J. F., Trentham, D. R., & Yates, D.,W. (1972) *Cold Spring Harbor Symp. Quant. Biol. 37*, 127−135.

Barshop, B. A., Wrenn, R. F., & Frieden, C. (1983) *Anal. Biochem. 130*, 134−145.

Boyer, P. D. (1993) *Biochim. Biophys. Acta 1140*, 215−250.

Capaldi, R. A., Aggeler, R. J., Turina, P., & Wilkens, S. (1994) *Trends Biochem. Sci. 19*, 284−289.

Cross, R. L. (1988) *J. Bioenerg. Biomembr. 20*, 395−405.

Eckstein, F. (1983) *Angew. Chem. 22*, 423−506.

Gogol, E. J., Lücken, U., Bork, T., & Capaldi, R. A. (1989) *Biochemistry 28*, 4709−4716.

Gogol, E. P., Johnston, E., Aggeler, R. J., & Capaldi, R. A. (1990) *Proc. Natl. Acad. Sci. U.S.A. 87*, 9585−9589.

Grubmeyer, C., Cross, R. L., & Penefsky, H. S. (1982) *J. Biol. Chem. 257*, 12092−12100.

Hammes, G. G. (1982) *Proc. Natl. Acad. Sci. U.S.A. 79*, 6881−6884.

Ishii, N., Yoshimura, H., Nagayama, K., Kagawa, Y., & Yoshida, M. (1993) *J. Biochem. (Tokyo) 113*, 245−250.

Jencks, W. P. (1980) *Adv. Enzymol. Relat. Areas Mol. Biol. 51*, 75−106.

Läuger, P. (1984) *Biochim. Biophys. Acta 779*, 307−341.

Penefsky, H. S. (1977) *J. Biol. Chem. 252*, 2891−2899.

Roberts, D. V. (1977) *Enzyme Kinetics*, Cambridge University Press.

Senior, A. E. (1990) *Annu. Rev. Biophys. 19*, 7−41.

Tanford, C. (1983) *Annu. Rev. Biochem. 52*, 379−409.

Thompson, R. C., & Karim, A. M. (1982) *Proc. Natl. Acad. Sci. U.S.A. 79*, 4922−4926.

Turina, P., & Capaldi, R. A. (1994) *J. Biol. Chem. 269*, 13465−13471.

Webb, M. R., Grubmeyer, C., Penefsky, H. S., & Trentham, D. R. (1980) *J. Biol. Chem. 255*, 11637−11639.

Weber, J., Wilke-Mounts, S., Lee, R. S.-F., Grell, E., & Senior, A. E. (1993). *J. Biol. Chem. 268*, 20126−20133.

Wilkens, S., & Capaldi, R. A. (1994) *Biol. Chem. Hoppe-Seyler 375*, 43−51.

Wise, J. G., Latchney, R. L., & Senior, A. E. (1981) *J. Biol. Chem. 256*, 10383−10389.

Wise, J. G., Duncan, T. M., Latchney, L. R., Cox, D. N., & Senior, A. E. (1983). *Biochem. J. 215*, 343−350.